Water vapor permeability of polymeric packaging materials for novel glass-free photovoltaic applications

Babin, Markus; Eder, Gabriele C.; Voronko, Yuliya; Oreski, Gernot

Published in:
Journal of Applied Polymer Science

Link to article, DOI:
10.1002/app.55733

Publication date:
2024

Document Version
Publisher's PDF, also known as Version of record

Received: 4 February 2024 | Revised: 1 May 2024 | Accepted: 9 May 2024

DOI: 10.1002/app.55733

RESEARCH ARTICLE

Applied Polymer SCIENCE WILEY

Water vapor permeability of polymeric packaging materials for novel glass-free photovoltaic applications

Markus Babin[1,2] | **Gabriele C. Eder**[2] | **Yuliya Voronko**[2] | **Gernot Oreski**[3]

[1]Institute for Electrical and Photonics Engineering, Technical University of Denmark, Roskilde, Denmark

[2]Austrian Research Institute for Chemistry and Technology, Wien, Austria

[3]Polymer Competence Center Leoben GmbH, Leoben, Austria

Correspondence
Markus Babin, DTU Electro, Frederiksborgvej 399, b. 130, 4000 Roskilde, Denmark.
Email: marbab@dtu.dk

Funding information
Österreichische Forschungsförderungsgesellschaft, Grant/Award Number: FO999897443

Abstract

Moisture ingress in photovoltaic (PV) modules is a critical factor for performance degradation, therefore, a low water vapor transmission rate (WVTR) is highly desirable for polymers used to embed the solar cells, including backsheets, frontsheets, and encapsulants. With the advent of glass-free modules for integration in building envelopes and vehicles, there is growing interest in polymer composite structures with embedded glass fibers to enhance rigidity. Furthermore, due to environmental concerns, there is increased interest in fluorine-free polymers for PV applications. In this work, 21 samples with different base polymers, coatings, and/or surface treatments are investigated and their WVTRs are measured. The results show no good alternatives to existing fluoride-based polymers/coatings for reducing WVTRs of backsheets and frontsheets among the investigated samples. In addition, glass fibers embedded within polymers to provide increased stability to backsheets or in composites for lightweight PV are shown to significantly increase WVTRs, especially, when fibers are not properly embedded, providing additional diffusion pathways for moisture ingress.

KEYWORDS

characterization, photovoltaics, WVTR

1 | MOTIVATION AND BACKGROUND

Solar photovoltaic (PV) electricity generation relies on light absorption within semiconductor materials. Since both the solar cells themselves, which are made up of several layers of semiconductor materials, and their electrical connections are susceptible to corrosion when exposed to moisture, protection is required.[1] Combined with the limited mechanical stability of the thin solar cells and the need for electrical insulation, this requires encapsulation of the power-generating parts (solar cells + connectors) within the PV modules.

This is best achieved using transparent and elastic polymer films, usually made of ethylene vinyl acetate (EVA) or polyolefin, which surrounds the cell strands and form the central and active part of the PV module laminate. Traditional PV module designs use glass as a front cover, which acts as an environmental barrier and provides structural integrity to the module without compromising solar transmittance. On the back, either another glass pane or a multilayer polymer film provides protection from environmental influences. Core layers

made of polyethylene terephthalate (PET) with thin fluorinated polymer films as protective inner and outer layers have been used as backsheets for decades. As alternatives, pure PET-based backsheets with or without coatings, as well as polyolefin and polyamide (PA) based materials, have been developed.[2–6]

Recently, glass-free modules have been gaining popularity in building integration (BIPV) as well as vehicle integration (VIPV) due to reduced weight and/or greater flexibility of shape. Instead of glass, a transparent polymeric frontsheet is used as the front cover of these PV modules. The main requirements for this frontsheet are high solar transmittance and high durability, considering UV exposure over several decades. The main materials used are fluoropolymers, mostly ethylene tetrafluoroethylene (ETFE)[7] and fluorinated ethylene propylene (FEP), with PET-based frontsheets containing fluoride-based layers or coatings representing lower cost alternatives.[2,8,9] Other materials like polycarbonate (PC) or polymethylmethacrylate (PMMA) have also been tested but showed reliability problems.[10–12]

The reasons for using fluoropolymers for back- and frontsheets are their high chemical- and temperature-resistance, stability under UV light and weathering as well as being good electrical insulators (due to low water absorption). Their high chemical stability and very high inertness, however, also result in long environmental persistence, a characteristic that is undesirable.[13] In 2023, the European Chemicals Agency (ECHA) has therefore proposed the ban of per- and polyfluorinated alkyl substances (PFAS).[14] While temporary exceptions are planned for applications without viable alternatives, harsher restrictions are to be expected in the long run, incentivizing the development of nonfluorinated polymers for use in PV. In addition, the high relative cost of fluoropolymers is driving interest from PV manufacturers in fluoride-free frontsheets in order to reach competitive module costs for glass-free module designs.[2]

An additional challenge for the construction of glass-free PV modules is the absence of a structural component providing rigidity and mechanical stability, which is of high importance, especially when using nonflexible semiconductor materials, such as crystalline silicon. Most designs for lightweight modules therefore rely on some kind of structural reinforcement, either included within the module laminate or provided externally, as shown in Figure 1. Internal reinforcement can be achieved through the inclusion of glass fiber mats within the module laminate, typically in the encapsulant behind the PV cells to avoid cell shading, as well as in the backsheet.[15,16] External reinforcement often relies on 3-dimensional polymeric composite structures, such as honeycomb sandwiches, to which the semiflexible PV modules are glued after lamination. Alternatively, the backsheet may be replaced directly by the top skin layer of the reinforcing composite.[9,17–19]

In this paper, we focus on the moisture barrier properties of different polymeric materials for use in glass-free PV modules, including fiber-reinforced skins as well as candidates for replacing PFAS-based polymers in encapsulants, frontsheets, and backsheets.

1.1 | Parameters and standards

Moisture barrier properties of polymeric materials are commonly assessed using measurements of the water vapor transmission rate (WVTR). It specifies the amount of water transmitted through a material when facing a constant moisture gradient and at a specific temperature. The measurement ranges for both humidity gradient and temperature vary significantly between scientific fields and measurement devices. Common values include 85%–0%RH or 50%–0%RH for humidity and 23, 37.8°C (=100°F) and 45°C for temperature. In these commonly measured temperature ranges, WVTR shows an exponential dependency on temperature according to the Arrhenius model.[20] In some studies, WVTR measurements have been performed at temperatures up to 85°C.

Guidelines for measuring WVTR of polymers are specified in ASTM F 1249 and ISO 15106-X for a variety of detection methods. While these standards do not

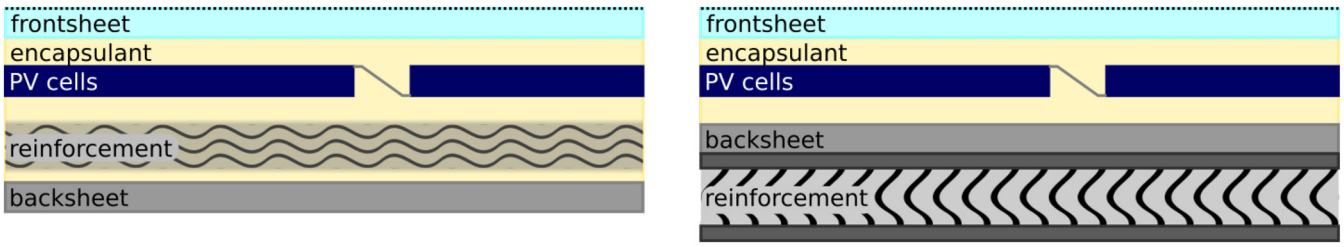

FIGURE 1 Types of structural reinforcement for glass-free modules: internal reinforcement (left) and external reinforcement (right). [Color figure can be viewed at wileyonlinelibrary.com]

mandate a specific humidity gradient, most measurements following them are performed at a humidity gradient of around 75%–90%RH.[21] For PV applications, the relevant standard IEC 62788-6-2 does not specify humidity gradients or temperatures.[22]

In general, the WVTRs of most materials follow Fick's laws of diffusion, which assuming steady state, leads to Equation (1), where P is the coefficient of permeation, Δp is the partial pressure difference for the permeant (in this case water vapor), and l is the thickness of the medium.[23]

$$WVTR = \frac{P \cdot \Delta p}{l} \tag{1}$$

The coefficient of permeation shows a dependency on temperature according to the Arrhenius model, described by the activation energy of the permeation process E_a:

$$P = P_0 \cdot e^{\frac{-E_a}{R_S T}} \tag{2}$$

Standard units for WVTR are (g/m^2/d), regardless of sample thickness, measurement temperature, and humidity differential. This makes the comparison of measured WVTR values inherently difficult, as they are significantly affected by these parameters. WVTR is frequently considered a bulk material property, samples of any known thickness can be measured and related to these standard units.

1.2 | Water permeation process

Jing et al.[24] separated the water permeation process into four main steps:

1. Adsorption of water molecules on the material surface.
2. Dissolution of water molecules over the material surface.
3. Diffusion of water molecules through the material.
4. Desorption of water molecules from the other material surface.

Steps 1 and 3 are affected by two distinct material properties: The hydrophilic nature of the material surface, which promotes water adsorption, and the porosity and polarity of the bulk material, which affect molecular diffusion. Polar polymers, or polymers with polar functional groups, show significantly higher WVTRs than nonpolar polymers, due to the higher solubility of water molecules.[25]

In composite materials made up of multiple (thin) layers, the layer with the lowest water diffusivity will predominantly affect the diffusivity of the entire composite.[26] In cases where the water permeation process is mainly limited by this diffusivity, this layer will therefore also determine the WVTR.

1.3 | Previous research

Multiple studies have investigated WVTR of PV materials—or base polymers with (potential) applicability in PV module encapsulation—as well as the phenomenon of moisture ingress in PV modules in general:

Dhere[27] published measurements performed at NREL (compare[28]) for various polymeric materials. Measurements were carried out using a Mocon Permatran-W 3/31 instrument at various temperatures ranging from 19 to 88°C. At 23°C, the materials showed a large spread of WVTRs, ranging from 1×10^{-3} to 1×10^{2} g/m^2/d for a thickness of 1 mm.

Kempe[29] also reported on moisture ingress in PV modules, showing that the high WVTR of EVA can lead to significant moisture ingress even in glass–glass modules over their lifetime. Kempe et al. subsequently investigated moisture ingress through module edges as well as WVTRs of edge sealants.[30,31]

Hülsmann et al.[20] measured WVTRs of several PV backsheet and encapsulant materials using a custom-built device with a mass spectrometer for detection of transmitted moisture.[32] For backsheet materials with a thickness of 1 mm, the measured WVTRs fell in the range of 1×10^{-3} to 1×10^{-1} g/m^2/d at a humidity gradient of 90%RH.

Hülsmann and Wallner[33] further investigated PET films used as a core or outer layer in PV backsheets, encompassing both transparent and white materials with varying stabilization. By investigating the relationship between film thickness, measurement temperature, and WVTR, they proposed the following modified equation:

$$WVTR = P_0 \cdot e^{\frac{-E_p}{R_S T}} \cdot \Delta p \cdot d^b \tag{3}$$

Hülsmann and Weiss[34] also presented a method to calculate the amount of moisture present in PV modules after accelerated aging tests, showing that water concentration in the PV encapsulant tends to reach an equilibrium concentration after several years, depending on climatic conditions.

Slapsak et al.[35] developed a device for in situ monitoring of moisture ingress in PV modules with which they were able to show that the microclimatic conditions in

the installation location have a large effect on humidity ingress and equilibrium concentration. They also proved the high accuracy of the Fickian diffusion model for common PV materials, validating moisture ingress simulations.[36]

Voronko et al.[5] could show that strong deviations in the aging-induced changes in the permeation rates of water vapor and oxygen can be correlated with the module performance. The rates of permeation of oxygen (OTR) and water vapor (WVTR) were determined on six types of backsheets in the original and artificially aged state (after 2000 h exposure time). The electrical power of test modules comprising the same backsheets was also determined before and after DH exposure.

1.3.1 | Influence of experimental conditions

As described in Section 1.1, the WVTRs of materials show a strong dependence on temperature and pressure gradient.

Hülsmann and Wallner reported activation energies of 34.1–37.1 kJ/mol for seven different PET layers, including both transparent and pigmented (white) materials designed for both core and outer layers, with different degrees of stabilization.[33] In a different article, the same authors reported activation energies of 33.9–35.6 kJ/mol for commercial backsheet samples with PVF-PET-PVF construction, as well as 35.4 kJ/mol for a three-layer PET backsheet.[20] This indicates that the temperature behavior of the WVTR is mostly a property of the core layer, or at least that PVF coatings have little influence on temperature dependency.

WVTRs of PET materials reported by Dhere showed significantly lower activation energies, ranging from 23.9 to 24.7 kJ/mol, however, the concentration gradient across the material layer was not reported.[27] Conversely, Jorgensen et al. reported much higher activation energies of 53.1 kJ/mol for WVTR through an uncoated PET film and 42.5 kJ/mol for WVTR through a PET film with well-performing coating.[37]

2 | SAMPLES AND MEASUREMENTS

2.1 | Sample selection

Three categories of samples are investigated, each containing established materials for PV applications as well as novel materials under development:

2.1.1 | Backsheets and skin layers

PV backsheets are commonly constructed from three layers. Typically, a PET core is surrounded by an external barrier layer for environmental protection and an internal layer for improved adhesion to the encapsulant. Traditionally, PVF has been used for both surrounding layers (backsheets known under the name Tedlar™), however, due to high costs and the overall aim to reduce PFAS, the PV industry is transitioning to alternative materials as already pointed out in the motivation part.

For lightweight PV modules, in which the front cover glass is replaced by a transparent polymer frontsheet, additional structural integrity has to be provided at the rear of the module. This can for example be achieved by replacing the backsheet with a honeycomb structure covered by two skin layers. Therefore, also several possible skin materials for such a lightweight module construction are measured, including PET- and PP-based skins, some of which are fiber-reinforced to improve mechanical stability.

An overview of all measured samples in this category is shown in Table 1.

2.1.2 | Frontsheets

While PV frontsheets often feature a 2- or 3-layer construction with mostly a PET main layer coated on one or both sides, the requirement for high transmittance and high reliability limits material choice significantly. As mineral fillers cannot be added, they are restricted to using chemical additives for UV stabilization and/or UV absorption.[38] Modern, high-efficiency cells with good spectral response in the UV region further limit the use of UV absorbers, which can make it difficult to achieve material stability over the expected lifetime of PV modules (≥25 years).

For a list of tested materials see Table 2.

2.1.3 | Encapsulants

In general, WVTR is less important for encapsulants than for the other polymers in PV laminates, as they are typically not fully exposed to the environment and therefore do not act as primary moisture barriers. Nevertheless, very high WVTRs are undesirable as that would facilitate water ingress at the edges of PV modules, especially, in the case of frameless modules or modules without edge sealing.

Most common types of PV encapsulants are based on either EVA or polyolefin (PO). Two main types of

TABLE 1 Measured backsheets/skins.

Name	Polymer	Thickness (μm)	Notes
B_PET_PE	PET + PE	370	Standard PET-based backsheet with PE coating on inside
B_PPGFa	PP	400	PP with embedded glass fibers (2-layers cross-ply)
B_PPGFb	PP	470	PP with embedded glass fibers (2-layers cross-ply)
B_PPGFc	PP	560	PP with embedded glass fibers (2-layers cross-ply)
B_PPGF6	PP	1300	PP with embedded glass fibers (6-layers cross-ply)
B_PPCF6	PP	1020	PP with embedded carbon fibers (6-layers cross-ply)
B_BOPET	PET	250	Corona-treated BOPET
B_PETgGF	PET	500	PETg with embedded glass fibers (2-layers cross-ply)
B_EP	Epoxy	480	Epoxy
B_EPGF	Epoxy	840	Epoxy with embedded glass fibers (1-layer)

Abbreviations: PE, polyethylene; PET, polyethylene terephthalate; PP, polypropylene.

TABLE 2 Measured frontsheets.

Name	Polymer	Thickness (μm)	Notes
F_PET_PU	PET + PU	286	PET layer with PU coating (front)
F_PET_ETFE	PET + ETFE	210	PET layer with ETFE coating (back)
F_PETa	PET	170	Uncoated PET layer
F_PETb	PET	124	Uncoated PET layer
F_PETa_X	PET	220	Coated PET
F_PETb_X	PET	184	Coated PET

Abbreviations: ETFE, ethylene tetrafluoroethylene; PET, polyethylene terephthalate; PU, polyurethane.

TABLE 3 Measured encapsulants.

Name	Polymer	Thickness (μm)	Notes
E_EVA	EVA	380	Standard EVA encapsulant
E_TPOa	PO	470	PE-PEA copolymer
E_TPOb	PO	470	PE-PEA copolymer with UV-absorbing additives
E_POE1	PE	500	Polyolefin elastomer encapsulant
E_POE2	PE	450	Polyolefin elastomer encapsulant

Abbreviations: EVA, ethylene vinyl acetate; PE, polyethylene; PEA, poly(ethyl-acrylate); PO, polyolefin.

polyolefinic encapsulants are currently developed and entering the market: (i) thermoplastic polyolefins (TPOs) consisting of individual polymer chains and (ii) polyolefin elastomers (POEs), which are loosely cross-linked to a 3-dimensional network (comparable with EVA) during the lamination process.[39,40] For this study, encapsulants of all three groups are tested and compared, as shown in Table 3.

Both TPO samples consist of the same base material, a copolymer of polyethylene (PE) and poly(ethyl-acrylate) (PEA), with one featuring UV-absorbing additives to provide additional degradation stability. The two POE samples are based on PE, albeit likely mixed with different cross-linkers and other additives.

2.2 | Measurement procedure

The WVTR of all samples was measured using a Mocon Permatran-W 3/34H at 85%RH and 23°C on a sample area of 50 cm^2. Due to the nonhomogeneous surface morphology of some samples, 2–4 measurements were performed on independent sample specimens for each material. To be able to compare these results, all WVTR results are referenced to a sample thickness of 100 μm.

2.3 | Visible light microscopy

In addition to WVTR measurements, images of composite skin layer cross-sections are taken under visible light

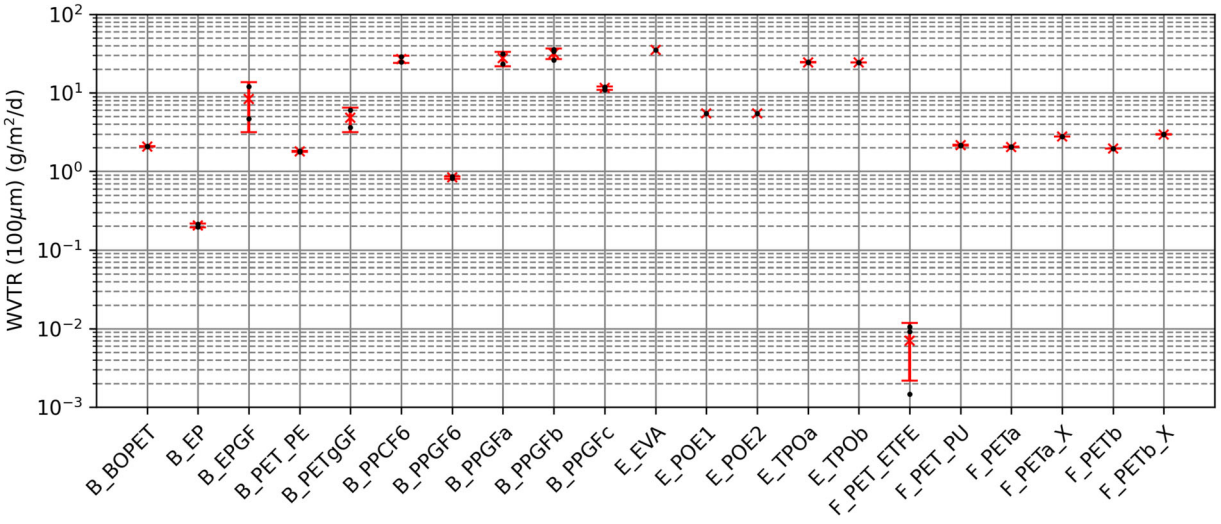

FIGURE 2 Overview of all water vapor transmission rate (WVTR) measurement results. [Color figure can be viewed at wileyonlinelibrary.com]

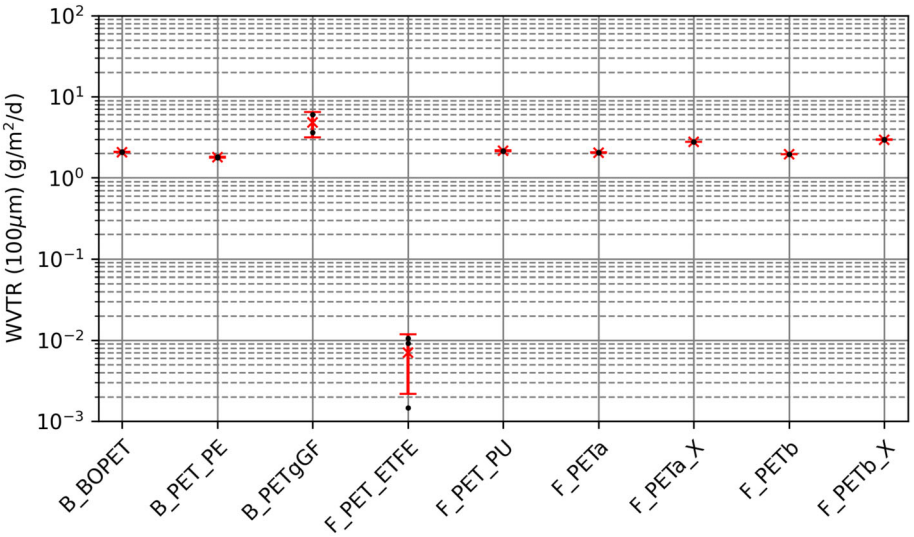

FIGURE 3 Water vapor transmission rate (WVTR) results for polyethylene terephthalate (PET)-based materials. [Color figure can be viewed at wileyonlinelibrary.com]

microscopy. To prepare samples, representative sections of the composite skins are embedded in epoxy resin and polished to allow imaging of the cross-sections.

3 | RESULTS AND DISCUSSION

An overview of all measured WVTRs is shown in Figure 2. The following sections show several trends that can be identified between material groups.

3.1 | Front and backsheets

Previous publications have shown that PET-based films without reinforcement exhibit WVTRs of around 1 $g/m^2/d$, while the presence of fluorine-based outer layers can reduce the value to circa 0.5 $g/m^2/d$.[5,41] PP-based multilayer backsheets typically show lower values around 0.1 $g/m^2/d$[4,42]

The results of all unmodified PET-based front and backsheets measured in this work show good agreement with these literature values, with WVTRs ranging from 1 to 3 $g/m^2/d$. Figure 3 shows the measured WVTRs of all PET-based materials, highlighting two outliers: the ETFE-coated PET frontsheet, which shows a very low WVTR and the PET skin layer with embedded glass fibers, with a higher WVTR. None of the other coatings or PET treatments have a significant effect on the WVTR, however.

The addition of glass fibers to the skin materials generally results in a significant increase in WVTR, a trend

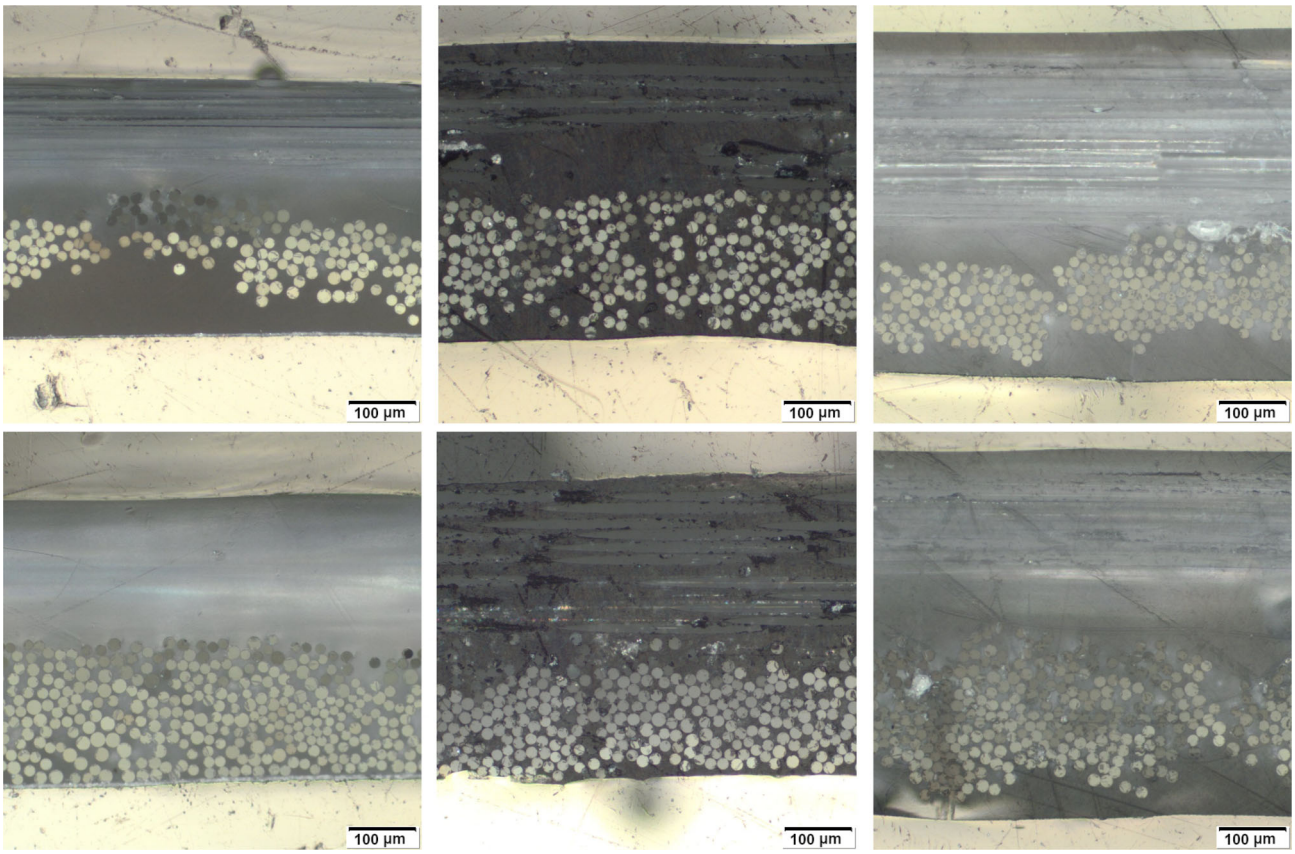

FIGURE 4 Visible light microscopy images for cross-sections of B_PPGFa, B_PPGFb, and B_PPGFc (left to right) for both fiber directions (top and bottom). [Color figure can be viewed at wileyonlinelibrary.com]

that can be observed for all embedding polymers. This can be attributed to advantageous diffusion pathways along the polymer-glass fiber interface.

Figure 4 shows visible light microscopy images for the three skins with 2-layer cross-ply embedded glass fibers, highlighting differences in fiber embedment. Cross-sections are shown for both fiber directions (top and bottom rows). Both B_PPGFa and B_PPGFb show poor covering of fibers near the laminate surface in at least one of the examined directions, while B_PPGFc shows good coverage of all fibers in both directions, with several micrometers of polymer material providing a smooth surface.

Referring to the WVTRs shown in Figure 2, it can be observed that in samples where fibers are reaching the surface of the laminates (e.g., B_PPGFa, B_PPGFb), the WVTR is significantly higher than in samples where the fibers are more properly embedded (e.g., B_PPGFc).

3.2 | Encapsulants

Measurements of encapsulants show significantly higher WVTRs compared with backsheet and frontsheet polymeric materials, as can be observed in Figure 5. Ranging from approximately 5.5 $g/m^2/d$ for the POE encapsulants to 35 $g/m^2/d$ for EVA, the differences between polymers can be explained by their respective polarity.

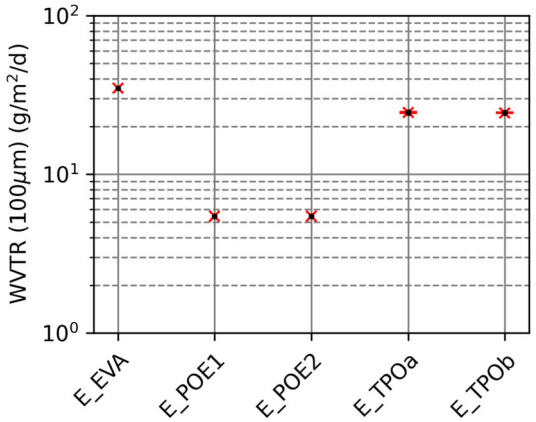

FIGURE 5 Water vapor transmission rate (WVTR) results for encapsulants. [Color figure can be viewed at wileyonlinelibrary.com]

Since the actual moisture ingress rate in a PV module is governed by the lowest WVTR in the laminate, it is

commonly determined by the backsheet materials, which show a WVTR that is 1–2 magnitudes lower than that of encapsulants. For moisture ingress through module edges where no backsheet is present, the difference between encapsulants becomes significant, however, favoring the use of POE encapsulants. This is especially relevant for glass–glass modules, where the edges represent the main moisture ingress site in PV modules. It is also relevant for product-integrated PV devices, where pathways for moisture ingress are short, and/or thin-film PV materials, which are especially sensitive to degradation in the presence of water.

3.3 | Repeatability and comparability

While most samples lead to repeatable measurement results, polymers with embedded fibers show significant variation between measurements, as shown through error bars. This is mainly due to the heterogeneous distribution of fibers within the material, which can lead to increased moisture penetration and diffusion, especially when poorly surrounded fibers reach the outside of the polymeric foil. As shown in Figure 4, the fibers tend to form bundled clusters, which lead to local variations in sample thickness and diffusion pathways for water transmission.

In this study, all WVTR results are referenced to a sample thickness of 100 µm, as it is intended to compare the performance of different materials and not the performance of specific products. To be able to compare these results, it is therefore essential to know the thickness of any sample of interest.

4 | CONCLUSION AND OUTLOOK

In this paper, WVTRs of samples consisting of different polymers, coatings, and/or treatments for use as PV backsheets, frontsheets, or encapsulants were measured to assess their suitability as moisture barriers in glass-free PV modules. Results for base materials were shown to be consistent with literature values, with polar polymers showing significantly higher WVTRs than nonpolar polymers.

The fluoride-free coatings for PET-based frontsheets did not show any significant reduction in WVTR compared with that of base PET, therefore no viable candidates for replacement of fluoride-based polymers/coatings could be identified. This highlights a continued, persistent gap in sustainable materials for use as transparent PV frontsheets. PP-based materials might be promising candidates, research in this regard is still ongoing.

Embedding of fibers within a polymer tends to lead to higher WVTRs, most likely caused by advantageous diffusion pathways along the polymer–fiber interface. Specifically, fibers that are covered by the embedding material and do not reach the surface generally result in a lower WVTR. The heterogeneous distribution of fibers within these samples also leads to a higher measurement uncertainty overall. This leads to the conclusion that homogeneously embedding fibers in sufficient amounts of the base polymer is critical when increasing the stability of backsheets or composite structures to provide rigidity to lightweight PV modules.

Following the characterization measurements presented here, test modules with selected skin and honeycomb materials based on PET and PP were manufactured and exposed to humid heat conditions in order to examine the moisture entry into the PV modules and the honeycomb structures in particular. The results are now being evaluated. In addition, aspects of recyclability have to be considered, such as minimizing the number of different materials and layers in front and backsheets.

AUTHOR CONTRIBUTIONS

Markus Babin: Investigation (equal); methodology (equal); validation (equal); visualization (equal); writing – original draft (equal); writing – review and editing (equal). **Gabriele C. Eder:** Conceptualization (equal); formal analysis (equal); investigation (equal); methodology (equal); validation (equal); writing – original draft (equal); writing – review and editing (equal). **Yuliya Voronko:** Investigation (equal); validation (supporting); writing – review and editing (equal). **Gernot Oreski:** Formal analysis (supporting); project administration (lead); validation (supporting); writing – review and editing (equal).

ACKNOWLEDGMENTS

The authors would like to acknowledge the funding support by FFG for the Solar-Era.Net Cofund project "Delight" (FFG, contract number FO999897443).

DATA AVAILABILITY STATEMENT

The data that support the findings of this study are available from the corresponding author upon reasonable request.

ORCID

Markus Babin https://orcid.org/0000-0002-1889-2540
Gabriele C. Eder https://orcid.org/0000-0003-0397-8453
Gernot Oreski https://orcid.org/0000-0003-4223-9047

REFERENCES

[1] O. K. Segbefia, A. G. Imenes, T. O. Sætre, *Sol. Energy* **2021**, *224*, 889.

[2] G. Oreski, J. Stein, G. Eder, K. Berger, L. Bruckman, J. Vedde, K.-A. Weiss, T. Tanahashi, R. French, S. Ranta, Designing New Materials for Photovoltaics: Opportunities for Lowering Cost and Increasing Performance through Advanced Material Innovations, Technical Report T13-13:2021, IEA PVPS Task 13. **2021**.

[3] A. Fairbrother, N. Phillips, X. Gu, *Durability and Reliability of Polymers and Other Materials in Photovoltaic Modules*, Elsevier, Amsterdam, Netherlands, **2019**, p. 153.

[4] G. Oreski, G. Eder, Y. Voronko, A. Omazic, L. Neumaier, W. Mühleisen, G. Ujvari, R. Ebner, M. Edler, *Sol. Energy Mater. Sol. Cells* **2021**, *223*, 110976.

[5] Y. Voronko, G. C. Eder, M. Knausz, G. Oreski, T. Koch, K. A. Berger, *Progr. Photovolt.: Res. Appl.* **2015**, *23*, 1501.

[6] C. Buerhop-Lutz, O. Stroyuk, T. Pickel, T. Winkler, J. Hauch, I. M. Peters, *Sol. Energy Mater. Sol. Cells* **2021**, *231*, 111295.

[7] S. L. Samuels, N. J. Glassmaker, G. A. Andrews, M. J. Brown, M. E. Lewittes, In 35th IEEE Photovoltaic Spec. Conf. IEEE, Honolulu, US, June **2010**, 002788–002790.

[8] H. Ng, In PV Reliability Workshop. **2020** 194–209 https://www.nrel.gov/docs/fy20osti/77317.pdf

[9] A. C. Martins, V. Chapuis, F. Sculati-Meillaud, A. Virtuani, C. Ballif, *Progr. Photovolt.: Res. Appl.* **2018**, *26*, 718.

[10] C. Schmid, E. Fuller, B. MacBride, R. Mickiewicz, G. Kinsey, J. Zhou, S. Chakravarti, A. Kodis, In 28th Eur. Photovoltaic Sol. Energy Conf. Exhib, Paris, France, October **2013**, 3090–3092.

[11] A. Backes, N. Adamovic, U. Schmid, In 28th Eur. Photovoltaic Sol. Energy Conf. Exhib, Paris, France, October **2013**, 3096–3098.

[12] K. Drabczyk, P. Sobik, Z. Starowicz, K. Gawlińska, A. Pluta, B. Drabczyk, *Microelectron. Int.* **2019**, *36*, 100.

[13] R. Lohmann, I. T. Cousins, J. C. DeWitt, J. Glüge, G. Goldenman, D. Herzke, A. B. Lindstrom, M. F. Miller, C. A. Ng, S. Patton, M. Scheringer, X. Trier, Z. Wang, *Environ. Sci. Technol.* **2020**, *54*, 12820.

[14] ECHA, ECHA Publishes PFAS Restriction Proposal. **2023** https://echa.europa.eu/-/echa-publishes-pfas-restriction-proposal

[15] J. Govaerts, B. Luo, T. Borgers, R. Van Dyck, A. Van Der Heide, L. Tous, A. Morlier, F. Lisco, L. Cerasti, M. Galiazzo, J. Poortmans, *EPJ Photovoltaics* **2022**, *13*, 13.

[16] B. Luo, J. Govaerts, R. Van Dyck, T. Borgers, B. Ruttens, M. C. Paesa, J. D'Haen, L. Tous, H. S. Radhakrishnan, M. Daenen, A. W. Van Vuure, J. Poortmans, *Sol. Energy Mater. Sol. Cells* **2023**, *259*, 112455.

[17] A. C. Martins, V. Chapuis, A. Virtuani, C. Ballif, *IEEE J. Photovolt.* **2019**, *9*, 245.

[18] A. C. Martins, V. Chapuis, A. Virtuani, H.-Y. Li, L.-E. Perret-Aebi, C. Ballif, *Sol. Energy Mater. Sol. Cells* **2018**, *187*, 82.

[19] J. Govaerts, P. Dufke, B. Luo, M. Bonnart, R. Van Dyck, T. Borgers, J. Poortmans, A. Derluyn, J. Saelens, W. Winant, M. Caliskan Arslan, U. Desai, F. Lisco, A. Faes, C. Ballif, G. Oreski, N. Pervan, G. Eder, 40th Eur. Photovoltaic Sol. Energy Conf., Exhib. Lisbon, Portugal, September **2023**, 020266–001–020266–006.

[20] P. Hülsmann, K.-A. Weiß, M. Köhl, *Progr. Photovolt.: Res. Appl.* **2014**, *22*, 415.

[21] C. Zerwas, International Permeation Measurement Standards. https://cobra-eng.nl/images/permeation_measurement_standards.pdf

[22] IEC TC82, Measurement procedures for materials in photovoltaic modules—Part 6-2: General tests—Moisture permeation testing of polymeric materials. EN IEC 62788-6-2:2020 **2020**.

[23] K. Lahtinen, J. Kuusipalo, presented at 11th TAPPI European PLACE Conf. **2007** 1023–1054.

[24] Z. Jing, Y. Guo, M. Ren, X. Zhao, H. Shao, Y. Zhou, M. Shuai, *e-Polym.* **2021**, *21*, 830.

[25] S. Marais, Q. T. Nguyen, C. Devallencourt, M. Metayer, T. U. Nguyen, P. Schaetzel, *J. Polym. Sci., Part B: Polym. Phys.* **2000**, *38*, 1998.

[26] S. Kiese, E. Kücükpinar, O. Miesbauer, H.-C. Langowski, *Thin Solid Films* **2019**, *672*, 199.

[27] N. G. Dhere, In Proceedings Volume 7048, Reliability of Photovoltaic Cells, Modules, Components, and Systems. **2008** 70480R.

[28] M. Kempe, 2004 DOE Solar Energy Technologies Program Review Meeting. **2005** www.nrel.gov/docs/fy05osti/37027.pdf

[29] M. D. Kempe, *Sol. Energy Mater. Sol. Cells* **2006**, *90*, 2720.

[30] M. D. Kempe, D. L. Nobles, L. Postak, J. A. Calderon, *Progr. Photovolt.: Res. Appl.* **2018**, *26*, 93.

[31] M. D. Kempe, A. A. Dameron, M. O. Reese, *Progr. Photovolt.: Res. Appl.* **2014**, *22*, 1159.

[32] P. Hülsmann, D. Philipp, M. Köhl, *Rev. Sci. Instrum.* **2009**, *80*, 113901.

[33] P. Hülsmann, G. Wallner, *Polym. Test.* **2017**, *58*, 153.

[34] P. Hülsmann, K.-A. Weiss, *Sol. Energy* **2015**, *115*, 347.

[35] J. Slapsak, S. Mitterhofer, M. Topic, M. Jankovec, *IEEE J. Photovolt.* **2019**, *9*, 1316.

[36] S. Mitterhofer, J. Slapšak, A. Astigarraga, D. Moser, G. O. Hernandez, P. V. Chiantore, W. Luo, Y. S. Khoo, J. Rabanal-Arabach, E. Fuentealba, P. Ferrada, M. Trigo Gonzalez, J. Ascencio-Vásquez, M. Topič, M. Jankovec, *IEEE J. Photovolt.* **2024**, *14*, 140.

[37] G. Jorgensen, K. Terwilliger, J. Delcueto, S. Glick, M. Kempe, J. Pankow, F. Pern, T. Mcmahon, *Sol. Energy Mater. Sol. Cells* **2006**, *90*, 2739.

[38] M. Aghaei, A. Fairbrother, A. Gok, S. Ahmad, S. Kazim, K. Lobato, G. Oreski, A. Reinders, J. Schmitz, M. Theelen, P. Yilmaz, J. Kettle, *Renewable Sustainable Energy Rev.* **2022**, *159*, 112160.

[39] G. Oreski, A. Omazic, G. C. Eder, Y. Voronko, L. Neumaier, W. Mühleisen, C. Hirschl, G. Ujvari, R. Ebner, M. Edler, *Progr. Photovolt.: Res. Appl.* **2020**, *28*, 1277.

[40] B. Adothu, F. R. Costa, S. Mallick, *Polym. Degrad. Stab.* **2022**, *201*, 109972.

[41] G. Oreski, A. Mihaljevic, Y. Voronko, G. C. Eder, *Polym. Test.* **2017**, *60*, 374.

[42] A. Omazic, G. Oreski, M. Edler, G. C. Eder, C. Hirschl, G. Pinter, M. Erceg, *J. Appl. Polym. Sci.* **2020**, *137*, 48899.

How to cite this article: M. Babin, G. C. Eder, Y. Voronko, G. Oreski, *J. Appl. Polym. Sci.* **2024**, e55733. https://doi.org/10.1002/app.55733